ELSEVIER

Journal of Photochemistry and Photobiology A: Chemistry 103 (1997) 143–152

Journal of PHOTOCHEMISTRY AND PHOTOBIOLOGY A:CHEMISTRY

Inclusion complexes of some 3H-indoles with cyclodextrins studied through excited state dynamics and steady state absorption and fluorescence spectroscopy

Shalini Nigam, Gilles Durocher *

Département de Chimie, Université de Montréal, C.P. 6128, Succ. Centre-ville, Montréal, Que., H3C 3J7, Canada

Received 8 July 1996; accepted 5 September 1996

Abstract

We present a steady state and time-resolved fluorescence study of two 3H-indole molecules, namely 2-[(*p*-amino)phenyl]-3,3-dimethyl-5-cyano-3H-indole (**1**) and 2-[(*p*-dimethylamino)phenyl]-3,3-dimethyl-5-cyano-3H-indole (**2**) in aqueous solutions of α-, β- and γ-cyclodextrins. The stoichiometries and association constants of the molecules have been assessed in the different cyclodextrin (CD) systems. The spectral characteristics, bandwidths and association constants show that molecule **2** experiences a stronger interaction with the host CDs than molecule **1**. Steady state fluorescence experiments show the presence of only one kind of complex for the molecules in α- and γ-CDs, whereas time-resolved fluorescence measurements and global analysis reveal the presence of two kinds of complex, thereby demonstrating the higher sensitivity of the time-resolved experiments. Fluorescence quenching is observed for both molecules in γ-CD, whereas in α- and β-CDs fluorescence enhancement is found. This has been correlated with the lower quantum yield of the complex in the former case. The observations of fluorescence quenching, together with the magnitudes of the association constants, show that the molecules form different complexes with γ-CD compared with α- and β-CDs.

Keywords: Cyclodextrins; Excited state dynamics; Inclusion complexes; 3H-Indoles; Steady state absorption and fluorescence spectroscopy

1. Introduction

Cyclodextrins (CDs) are water-soluble cyclic oligosaccharides which form hydrophobic cavities with hydrophilic external walls [1,2]. With their toroidal shape and relatively apolar interior, CDs can selectively incorporate molecules on the basis of size and polarity characteristics to form inclusion complexes; this has led to the widespread utilization of CDs in the pharmaceutical, food, cosmetic and other chemical industrial areas [2–5]. CDs have been suggested as enzyme mimics [6] and as models of protein–ligand interaction [7]. Hydrophobic forces and van der Waals' interactions are considered to be the major forces involved in inclusion complex formation. The commonly available CDs are α-, β- and γ-CDs containing six, seven and eight glucopyranose units respectively with inner cavity diameters of 5.7, 7.8 and 9.5 Å. These cavities open at the primary and secondary hydroxyl faces of the cyclic sugar network.

The inclusion of organic and organometallic compounds within the CD hydrophobic cavity and its effect on the photophysical properties of these molecules have been the subject of many investigations [8–36]. These properties include fluorescence enhancement [8–14], intramolecular excimer/exciplex formation [15–18], twisted intramolecular charge transfer (TICT) phenomena [19–22], fluorescence quenching phenomena [23–26] and excited state intramolecular proton transfer reactions [27,28]. The restrictive shape and size of the CDs also prompt changes in the excited state geometry [22,29–31]. The complexed molecules can be included wholly or partially in the CD cavity, and many studies have focused on the ability of CDs to include guests of varying size in different stoichiometric ratios [32–36]. Depending on the size of the host CD (α-, β- or γ-CD) and the size of the guest molecule, different guest to host stoichiometries are possible. A correct evaluation of the stoichiometry of the complex is crucial for the accurate determination of the formation constant, and an examination of this value can provide a clearer understanding of the factors affecting complexation.

In the last few years, we have been interested in examining substituted 3H-indoles in different homogeneous and heterogeneous environments [37–46]. It has been shown that

* Corresponding author.

PII S1010-6030(96)04488-7

these molecules are not rigid and that the phenyl ring can librate within the kT energy barrier [37,39]. This torsional motion is responsible for the geometric changes which take place in the ground and excited states and provides an important deactivation pathway. It has been observed that the spectroscopy and photophysics of these 3H-indoles are largely influenced by the nature of the substituents in the para position of the phenyl ring [38]. These molecules are sensitive to their environment and thus can act as probes in the study of microstructures [43–46].

Previously, we have studied the behaviour of 2-[(*p*-amino)-phenyl]-3,3-dimethyl-5-cyano-3H-indole (**1**) and 2-[(*p*-dimethylamino)phenyl]-3,3-dimethyl-5-cyano-3H-indole (**2**) in β-CD and observed that they form inclusion complexes with two different well-defined stoichiometries, i.e. 1 : 1 and 2 : 1 (β-CD : substrate) [46]. In this paper, we present a comparative study of these molecules in all three α-, β- and γ-CDs, and demonstrate that it is the size of the host CD which affects the behaviour of the probe molecules in the different host CDs.

2. Experimental details

2.1. Materials

The synthesis and purification of the two molecules (see Fig. 1) were performed according to the modified methods of Skrabal et al. [47] (reported in the M.Sc. thesis of A. Popowycz [48]). Analytical grade reagent sodium hydroxide, sulphuric acid and methanol were used as received. β-CD (Aldrich) was recrystallized twice using deionized triply distilled water and dried under vacuum. α- and γ-CDs (Aldrich) were used as received. Deionized triply distilled water was used to prepare the solutions.

2.2. Instruments

Absorption spectra were recorded on a Philips PU 8800 UV–visible spectrophotometer. Corrected fluorescence spectra were measured on a Spex Fluorolog-2 spectrofluorometer with an F2T11 special configuration. Fluorescence lifetimes were determined on a multiplexed time-correlated single-photon counting fluorometer (Edinburgh Instruments, model 299T). The time resolution of the system after deconvolution was 0.1 ns.

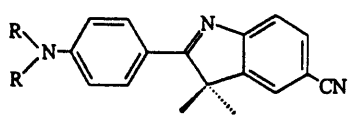

1 R = H
2 R = CH_3

Fig. 1. Molecular structures of 2-[(*p*-substituted)phenyl]-3,3-dimethyl-5-cyano-3H-indoles.

2.3. Methods

Fresh sample solutions were used in the absorption and fluorescence measurements. Stock solutions of the α-, β- and γ-CDs were prepared with distilled water and dilutions were made from these stock solutions to obtain the different desired concentrations. When preparing the CD solutions, the pH was maintained by adding NaOH and H_2SO_4 and no buffers were used. Stock solutions of **1** and **2** were prepared in methanol, and 0.1 ml aliquots of these stock solutions were added to the CD solutions to maintain the final concentrations of both molecules in the range $(2–4) \times 10^{-6}$ M. The absorption and fluorescence spectra and lifetimes of molecules **1** and **2** were checked in the presence and absence of methanol to determine the possible influence of the alcohol in complexation. It was found to have no effect. Isosbestic points were used for excitation to calculate the association constants. The fluorescence quantum yields were measured using the DM3H molecule [37] as a standard in methanol ($\phi = 0.24$). To analyse the lifetime data at different concentrations and fluorescence wavelengths, a global iterative re-weighted reconvolution program based on a non-linear, least-squares method was used (Globals Unlimited, Urbana, IL) [49] (based on the Marquardt algorithm [50]). The entire decay profiles were analysed at different concentrations of the CD solutions and, in the case of γ-CD, at different emission wavelengths. Lifetime data were both individually and globally analysed using single, double and triple exponentials.

3. Results and discussion

3.1. Spectral characteristics

The absorption spectra of molecules **1** and **2** (Fig. 1) are very different in the three CD systems. When the concentrations of the three CDs are increased, small red shifts are observed, with a small change in the extinction coefficients of the two molecules in β-CD. These changes are hardly apparent in α-CD and the observed isosbestic points are scattered. For γ-CD, the shifts are very slight, but there is a significant change in the band shape with respect to water and the other CDs (Fig. 2). For molecule **2**, a large increase in the extinction coefficient is observed (Table 1), and a shoulder appears at the red edge of the absorption band (approximately 440 nm). This is not observed in any other CDs or in water.

The 3H-indole molecules are stabilized in polar solvents by hydrogen bonding involving the tertiary nitrogen atom. For these molecules, the absorption energy decreases on moving from non-polar to polar protic solvents [37–39]. However, this energy increases from methanol to water and is attributed to an additional hydrogen bonding interaction involving the terminal nitrogen atom electron lone pair [40,41]. Water acts as a hydrogen bond donor to the lone pair of the terminal nitrogen atom, causing reduced conju-

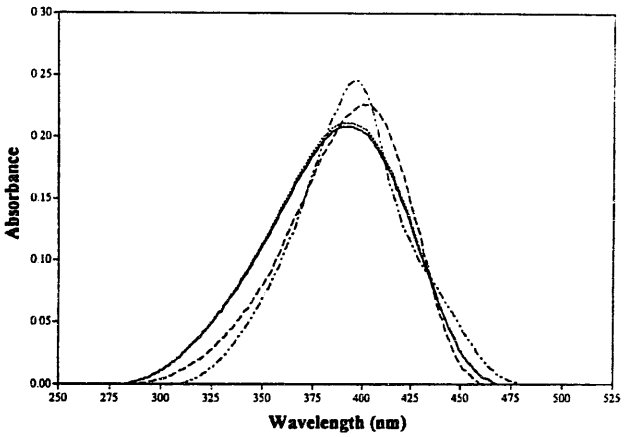

Fig. 2. Absorption spectra of molecule **2** in water (———), α-CD (· · ·), β-CD (– – –) and γ-CD (– · · –). [CD] in all cases is 0.004 M.

gation of the phenyl ring with the indole moiety. As the concentrations of the CDs are increased, the red shifts concurrent with a decrease in the bandwidth indicate that both molecules form complexes with the CDs in which the molecules experience a reduced polarity compared with that in water. The changes are hardly apparent in α-CD, suggesting that the interaction between α-CD and the molecules is very weak. In γ-CD, the changes are well defined and two clear isosbestic points are observed at all concentrations.

The fluorescence changes are rather interesting. An increase in the fluorescence intensity is observed, together with negligible changes in the energy of molecules **1** and **2**, in α-CD, in much the same way as in β-CD [46]. However, the changes are much less pronounced than with β-CD. The fluorescence bandwidths, fluorescence lifetimes and quantum yields of the two molecules are increased in α-CD and the Stokes shift is decreased, confirming the lower polarity of the CD cavity. For these 3H-indole molecules, the fluorescence quantum yields and lifetimes are controlled solely by the non-radiative rate parameter [42]. In pure water and acidic media, the strong fluorescence quenching of these molecules has been attributed to the occurrence of a TICT radiationless channel on the basis of theoretical and experimental results [40–42]. In the α- and β-CD complexes, the non-radiative rate parameters or the ϕ_f values are close to those observed in methanol–water mixtures [44–46], indicating that the molecules on average are close to the alcoholic hydroxyl rim.

Unlike in α- and β-CDs, the fluorescence intensities of molecules **1** and **2** are quenched in the presence of γ-CD. As the concentration of γ-CD is increased, a red shift of the order of 8–12 nm is observed, together with a broadening of the fluorescence band and a decrease in the fluorescence intensity (Fig. 3). This is accompanied by an increase in the Stokes shift and a clear isoemissive point. These results are very unusual in the sense that the fluorescence maxima of the molecules are not very sensitive to the polarity [42]. This leads to the conclusion that molecules **1** and **2** form inclusion complexes with γ-CD, whose characteristics are very different from those of the complexes formed with α- and β-CDs. We can rule out the formation of excimers of **1** and **2** because, on checking the fluorescence characteristics at low and high concentrations of the molecules, no change in the trend with regard to the wavelength shifts and fluorescence quenching was observed. The formation of exciplexes between **1** and **2** and γ-CD can also be eliminated on the basis of kinetic data (see Table 4), where no negative pre-exponential factors are observed. The occurrence of 2 : 1 (3H-indole : γ-CD) complexes must also be ruled out since, on varying the concen-

Table 1
Spectral characteristics and quantum yields of molecules **1** and **2** in water, α-CD and γ-CD at 298 K

Molecule	Medium	ν_A^a (cm^{-1})	ϵ^b (M^{-1} cm^{-1})	ν_F^c (cm^{-1})	Stokes shift (cm^{-1})	FWHM(abs) (cm^{-1})	FWHM(flu) (cm^{-1})	ϕ_F
1	Water, pH 9.5	28 000	33 000	21 100	6900	5700	3000	0.052
	α-CD, 0.001 M, pH 9.5	28 000	33 000	21 100	6900	5700	3000	0.054
	α-CD, 0.01 M, pH 9.5	27 600	33 000	21 000	6600	5700	3100	0.073
	γ-CD, 0.0004 M, pH 9.5	28 000	33 000	21 000	7000	5400	3000	0.046
	γ-CD, 0.004 M, pH 9.5	27 900	33 000	20 700	7200	4800	3400	0.031
2	Water, pH 9.5	25 600	39 200	20 200	5400	5200	2600	0.03
	α-CD, 0.001 M, pH 9.5	25 600	39 200	20 200	5400	5200	2600	0.033
	α-CD, 0.01 M, pH 9.5	25 300	39 200	20 200	5100	5100	2600	0.045
	γ-CD, 0.0004 M, pH 9.5	25 600	43 500	20 000	5600	5100	2900	0.026
	γ-CD, 0.004 M, pH 9.5	25 200	46 300	19 500	5700	3800	3200	0.024

[a]Absorption wavenumbers taken at the centre of mass of the absorption band. [b]Absorptivity coefficient at the peak intensity maximum. [c]Fluorescence wavenumbers taken at the centre of mass of the fluorescence spectrum.

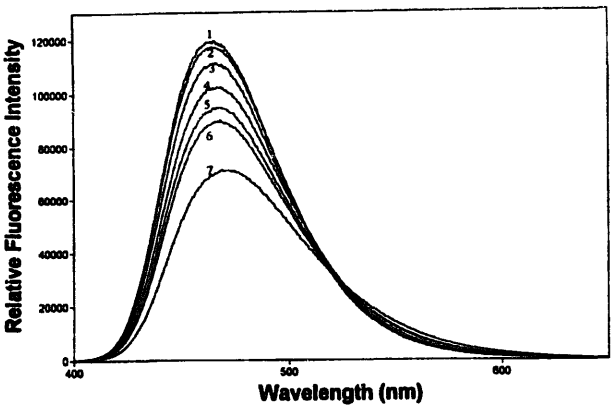

Fig. 3. Fluorescence spectra of molecule 1 at different concentrations of γ-CD: 1, 0 M; 2, 10^{-4} M; 3, 4×10^{-4} M; 4, 8×10^{-4} M; 5, 10^{-3} M; 6, 2×10^{-3} M; 7, 10^{-2} M (λ_{exc} = 375 nm).

Table 2
Effect of excitation wavelength on the emission wavelength maxima for molecules 1 and 2 in γ-CD ([CD] = 0.004 M)

Molecule 1		Molecule 2	
λ_{exc} (nm)	$\lambda_{emission}$ (nm)	λ_{exc} (nm)	$\lambda_{emission}$ (nm)
380	476	380	500
400	477	400	501
420	484	420	498
430	488	430	498
440	503	450	502
445	509	460	502
450	515	470	503
455	515	475	505
460	516	480	506

trations of 1 and 2, no band characterizing higher order species was observed. With this information in hand, we checked the effect of the excitation wavelength on the emission characteristics of the molecules in the three CDs. We found that there is no red edge excitation effect for the molecules in α- and β-CDs; however, in γ-CD, we observed a very clear pattern for molecule 1 (see Table 2), for which the emission wavelength maximum moved towards the red side at higher excitation wavelengths. This pattern is not reproduced for molecule 2, even though a small red shift is observed. This observation, together with the fact that the absorption band shape changes with the addition of γ-CD (as discussed above), indicates that the molecules form complexes with γ-CD in such a way that many different conformations may exist, which together contribute to the broadened fluorescence spectrum. This kind of behaviour, in which different conformations of the molecule in different environmental conditions contribute to broaden the fluorescence spectrum, has been observed previously [51]. The decrease in the fluorescence intensity may be due to the fact that the quantum yield of the complex is low as a result of a decrease in the radiative decay rate and/or an increase in the radiationless decay rate. However, since the fluorescence lifetime increases in the presence of γ-CD (see Table 4), the fluorescence decay rate of the complexed species should decrease. This is opposite to the behaviour observed for the molecules in α- and β-CDs, where the fluorescence quantum yield increases. Thus the size of the CD cavity seems to be the driving force behind the different behaviour of the molecules in the different cavities.

3.2. Association constants

To obtain the ground state association constants from the fluorescence intensities and lifetimes of ground state species which form a reversible equilibrium described by the inclusion compound formation constant K, we must eliminate the identifiability problem [52]. The following discussion is based on the assumption that the composite decay rate constants of the various species are much higher than the first-order dissociation constants of each of the excited complexes. We believe that this assumption is reasonable in view of the small fluorescence lifetimes of the uncomplexed and complexed species.

For an analysis based on complexation, a knowledge of the association constants for CD complexes is necessary in order to predict and better understand the interactions between the CDs and the guests in solution. The association constant provides a measure of the complex stability and an understanding of the factors affecting the complexation. Briefly, for a simple 1 : 1 complex, where S is taken to represent the fluorescence substrate, the equilibrium can be written as

$$S + CD \rightleftharpoons SCD \quad (1)$$

The equilibrium constant K_1 is then expressed as

$$K_1 = \frac{[SCD]}{[S][CD]} \quad (2)$$

where [SCD] is the equilibrium concentration of the inclusion complex for a given CD concentration. The classical method for the determination of K_1 is the preparation of a double-reciprocal plot [53], derived from the following equilibrium equation

$$K_1 = \frac{[SCD]}{([S]_0 - [SCD])([CD] - [SCD])} \quad (3)$$

where $[S]_0$ and [CD] are the initial analytical concentrations of S and CD. In our study, the concentration of CD is large with respect to that of the complex, i.e. $[CD] \gg [SCD]$. Thus Eq. (3) becomes

$$K_1 = \frac{[SCD]}{([S]_0 - [SCD])([CD])} \quad (4)$$

The fluorescence intensity of S in the presence (I) and absence (I_0) of CD is proportional to [SCD] and [S] respectively [28]. The total fluorescence intensity observed from a substrate molecule in a CD solution then becomes the weighted average of the intensities from the free and complexed molecules. Thus

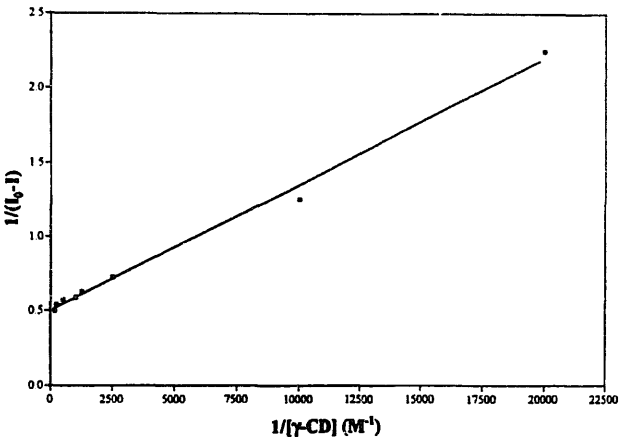

Fig. 4. Double-reciprocal plot for molecule **2** complexed to γ-CD at 298 K following the application of Eq. (6).

$$\frac{[SCD]}{[S]_0}=\frac{I_0-I}{I_0-I_1} \tag{5}$$

where I_0 and I_1 denote the fluorescence intensity in pure water and in the complex respectively and I is the fluorescence intensity at a given CD concentration. Combining Eq. (4) with Eq. (5), we obtain

$$\frac{1}{I_0-I}=\frac{1}{K_1(I_0-I_1)}\frac{1}{[CD]}+\frac{1}{I_0-I_1} \tag{6}$$

This implies that a Benesi–Hildebrand plot of $1/(I_0-I)$ vs. $1/[CD]$ should give a straight line; from the slope and intercept, we can estimate the values of K_1 and I_1.

Fig. 4 illustrates a double-reciprocal plot for molecule **2** in γ-CD. As can be seen, the plot is well described as a single straight line, from which the values of the association constants have been determined (Table 3). Similar plots were obtained for both molecules in α- and γ-CDs. This linear behaviour is contrary to that observed for these molecules in β-CD [46], where the plot is best described by two linear segments each giving a different association constant. This leads to the conclusion that molecules **1** and **2** form only one type of complex, i.e. 1 : 1, in α- and γ-CDs, whereas, in β-CD, two different types of complex are formed.

In Table 3, it can be seen that molecule **2** forms much stronger complexes than molecule **1** in γ-CD. This is in keeping with the more hydrophobic nature of molecule **2**, and has been observed previously when binding constants for these molecules were determined in sodium dodecyl sulphate (SDS) and cetyltrimethylammonium bromide (CTAB) micelles [44,45] and in β-CD [46]. The association constant of molecule **2** was found to be higher in SDS, CTAB and β-CD systems relative to that of molecule **1**. This has been related to the stronger hydrophobic interactions experienced by molecule **2** due to its larger volume (383 Å^3 compared with 332 Å^3 for molecule **1** [45]). When we compare the values of the association constants in the host CD systems, we see that they are very low in α-CD and highest in γ-CD. This shows that the interactions of the molecules are very weak with α-CD and strongest with γ-CD. Thus the sizes of both the CD cavity and the guest molecule seem to be the driving forces behind the complexation phenomena.

To date, detailed studies of the fluorescence enhancement phenomena of CDs and aromatic compounds have been reported, but few studies are available on the fluorescence quenching of compounds by CDs [23–26]. Patonay et al. [23] have proposed modified Stern–Volmer equations to explain the quenching behaviour of pyrene in CD solutions. According to Ref. [23], although the formation of a ground state dark complex is an obvious explanation for the quenching of the fluorophore, an equally plausible cause may be a decrease in the quantum yield of the complex. In fact, the formation of a dark complex can be considered as a special case of the quantum yield change. If we rearrange Eq. (6) in the form of a Stern–Volmer equation, we obtain

$$\frac{I_0-I}{I}=\frac{K_1[CD](I_0-I_1)}{I_0+I_1K_1[CD]} \tag{7}$$

If we define the change in the quantum yield of the complex compared with the quantum yield of the free system as d, then

$$d=\frac{I_1}{I_0} \tag{8}$$

Introducing this into Eq. (7), we obtain

$$\frac{I_0-I}{I}=\frac{K_1[CD](1-d)}{1+K_1[CD]d} \tag{9}$$

This equation is exactly the same modified equation as proposed by Patonay et al. [23] for the special case of the quantum yield change of the complex formed. If a dark complex is formed, then $d=0$, and we obtain the traditional Stern–Volmer equation and the plot should be linear. When we plotted the values of $(I_0-I)/I$ vs. the CD concentration, the data points followed a non-linear trend. This indicates that the quenching may not only be static or that the complex may also emit. However, since the average fluorescence lifetime (see Table 4) in the presence of CD increases, dynamic quenching does not seem to be operative here. We then plotted the same values taking the factor d into account according

Table 3
Association constants K_1 (dm^3 mol^{-1}) and K_2 (dm^3 mol^{-1}) of molecules **1** and **2** in α- and γ-CDs at 298 K

Molecule	Medium	K_1	K_2^c
1	α-CD	19[a]	
		21[b]	26
	γ-CD	1010[a]	
		1240[b]	16
2	α-CD	22[a]	
		17[b]	17
	γ-CD	5870[a]	
		7810[b]	40

[a]Determined by the double-reciprocal method provided by Eq. (6).
[b]Determined by the lifetime method provided by Eqs. (13) and (14).

to the modified Eq. (9), and used a non-linear regression analysis program [54] to determine the value of d. The fits converged very well with the data points with $r^2 = 0.98$ (see Fig. 5). The quantum yield change d for molecule **1** is 0.55 and for molecule **2** is 0.85. Thus the most probable explanation of the fluorescence quenching in γ-CD is the decreased quantum yield of the complex formed.

3.3. Lifetime measurements

The lifetimes of the molecules were measured at different concentrations of the different CDs. The excitation wavelengths were 360 nm and 370 nm and the emission wavelengths were 470 nm and 475 nm for molecules **1** and **2** respectively. A total of 10 000 counts were collected for each sample. The fluorescence decay profiles collected at various fluorescence wavelengths were fitted to the expression

$$I(t) = \sum_{i=1}^{n} B_i \exp(-t/\tau_i) \qquad (10)$$

where $I(t)$ is the intensity of the fluorescence at time t, B_i is the pre-exponential factor for that fraction of the fluorescence intensity, τ_i is the fluorescence lifetime of the emitting species and n is the total number of emitting species. The analysis was carried out using the Marquardt algorithm [50] which

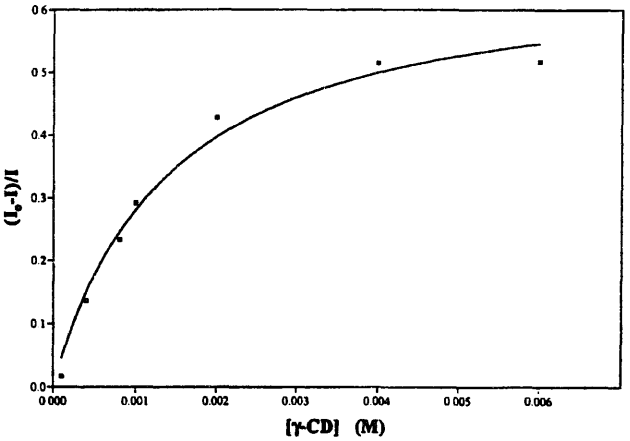

Fig. 5. Plot of $(I_0 - I)/I$ vs. [CD] for molecule **1** in γ-CD. The full line is the non-linear regression fit (Eq. (11)) to the experimental data points.

provides estimates of the values of the residuals, autocorrelation and reduced χ^2.

For both molecules in α-CD, the molecular decay curves could be fitted to double-exponential functions for all the concentrations studied. The curves were also fitted using triple-exponential analysis, but χ^2 did not improve. However, it was observed that the two components of the lifetime increased with increasing concentration. A global double-exponential analysis was carried out for both molecules at

Table 4
Lifetimes, normalized pre-exponential factors and the fraction f[a] associated with the decay for molecules **1** and **2** at different concentrations of α- and γ-CDs

Molecule	Medium	Concentration (M)	τ_1 (ns)	B_1	f_1	τ_2 (ns)	B_2	f_2	τ_3 (ns)	B_3	f_3	Individual χ^2	χ^2_g
1	α-CD	0	0.18	1.0	1.0	1.7	0	0	2.5	0	0	1.46	1.18
		0.001		0.99	0.91		0.01	0.09		0.	0	1.26	
		0.002		0.97	0.75		0.3	0.25		0	0	1.13	
		0.006		0.95	0.67		0.04	0.28		0.01	0.05	1.1	
		0.01		0.94	0.61		0.04	0.29		0.01	0.11	1.19	
		0.02		0.91	0.45		0.05	0.26		0.04	0.29	1.13	
		0.04		0.83	0.28		0.09	0.24		0.08	0.48	1.03	
2	α-CD	0	0.21	1.0	1.0	1.7	0	0	2.6	0	0	1.47	1.14
		0.001		0.93	0.66		0.07	0.34		0	0	1.01	
		0.002		0.93	0.64		0.07	0.35		0.01	0.01	1.11	
		0.006		0.90	0.52		0.08	0.37		0.02	0.11	1.13	
		0.01		0.87	0.43		0.1	0.39		0.03	0.18	1.11	
		0.02		0.78	0.28		0.15	0.43		0.07	0.29	1.12	
		0.04		0.71	0.2		0.17	0.38		0.12	0.42	1.11	
1	γ-CD	0	0.22	1.0	1.0	1.4	0	0	5.0	0	0	1.08	1.14
		0.0004		0.96	0.8		0.04	0.2		0	0	1.07	
		0.001		0.91	0.65		0.08	0.34		0.01	0.01	1.06	
		0.004		0.79	0.37		0.20	0.58		0.01	0.05	1.2	
		0.006		0.75	0.32		0.24	0.63		0.01	0.05	1.11	
		0.01		0.73	0.27		0.26	0.6		0.02	0.13	1.35	
2	γ-CD	0	0.19	1.0	1.0	1.4	0	0	4.2	0	0	1.15	1.1
		0.0001		0.96	0.74		0.03	0.16		0.01	0.1	1.13	
		0.0004		0.89	0.42		0.08	0.28		0.03	0.3	1.04	
		0.001		0.84	0.30		0.11	0.36		0.05	0.4	1.09	
		0.004		0.74	0.19		0.18	0.36		0.08	0.45	1.08	
		0.006		0.70	0.16		0.21	0.38		0.09	0.46	1.11	
		0.01		0.68	0.15		0.23	0.40		0.09	0.45	1.19	

[a] f_i is the fractional contribution from one species at one particular wavelength to the total fluorescence intensity defined as $f_i = (B_i\tau_i)/(\Sigma_i B_i\tau_i)$, where B is the pre-exponential factor and τ is the associated lifetime where $\Sigma f_i = 1$.

different concentrations of α-CD, ranging from 0 to 0.04 M, in much the same manner as for β-CD [47]. The lifetimes were linked together and the pre-exponential factors were allowed to float. The results were judged by the statistical fitting parameters χ^2 for the individual single curve analysis and for global analysis (χ^2_g). The statistical criteria for judging the quality of the fit included both graphical and numerical tests. The global reduced χ^2_g values were tabulated and used as a numerical test. The normal deviate $Z\chi^2_g$ [55] corresponding to χ^2_g is obtained from Eq. (11)

$$Z\chi^2_g = (\nu/2)^{1/2}(\chi^2_g - 1) \quad (11)$$

where ν is the number of degrees of freedom. $Z\chi^2_g$ is always less than 1.4 for our results. It should normally be less than 1.96 for a 95% confidence level in the fit [55].

The results of the above analysis indicate that two lifetimes are obtained, but the χ^2_g value is poor. Therefore we carried out a global triple-exponential analysis with the same data conditions; this led to a large improvement in the χ^2_g value and three lifetimes were observed with changing pre-exponential factors. The data listed in Table 4 show that the shortest component is close to the lifetime of the molecules in pure aqueous medium [43], and the longest component is close to the reported lifetime of the molecules in β-CD solution [46]. This analysis indicates the existence of two types of complex which could not be detected by steady state methods. In addition, the longest component only appears at higher concentrations of CD, but the shortest component has a significant contribution even at 0.04 M. This indicates that a certain number of molecules remain uncomplexed by the CD. Indeed, up to 0.01 M, the fraction of molecules in water is predominant, which indicates the extremely weak interaction between the molecules and α-CD. We have already shown the magnitude of this complexation by the calculation of the association constant (Section 3.2). Thus, unlike the complexes formed with β-CD, complex formation with α-CD is very weak.

For γ-CD, we measured the lifetimes in a similar manner to that described above. For molecule **1** in γ-CD, the fluorescence decay curves could be fitted to a double-exponential function at concentrations below 0.004 M; however, above this concentration, a triple-exponential curve was necessary. For molecule **2**, the curves could be fitted to a triple-exponential function at all concentrations, thereby showing that the interactions experienced with γ-CD are stronger than those for molecule **1**. On carrying out a global triple-exponential analysis of the two molecules over a wide concentration range, three lifetimes were obtained with changing pre-exponential factors and excellent values of χ^2_g. The shortest lifetime corresponds to the lifetime in pure aqueous medium [43], whereas the middle lifetime (approximately 1.4 ns) corresponds to the lifetime experienced by the 1 : 1 complex formed in β-CD [46]. The longest component of the lifetime is the anomalous behaviour here. Lifetimes of this order of magnitude have never been observed previously for these molecules in any medium [42–46]. Obviously this lifetime corresponds to a higher ordered structure, possibly a 2 : 1 complex. It should be noted that the contribution from the third component is very small for molecule **1**. In addition, even at the highest concentrations of the CD, there is a significant contribution from the smallest component, i.e. the molecule in water. This shows that some probe molecules are always present in the γ-CD solution in the free and uncomplexed form, and demonstrates that the interactions are different compared with those in β-CD where, at the highest concentrations taken, there is only a contribution from the highest lifetime species.

The above results show that there are at least two kinds of complex formed, one of which may be too weak to be detected by steady state measurements. Jobe et al. [34] have devised a method for the calculation of the association constants using the lifetime measurements. Since we were unable to calculate the association constant of the second complexed species using the steady state technique, we use their method to assess the second association constant. In addition to the equilibrium described by Eq. (1), we must consider the following equilibrium for which the equilibrium constant is K_2

$$SCD + CD \overset{K_2}{\rightleftharpoons} S(CD)_2 \quad (12)$$

Usually, K_1 can be calculated from Eq. (6), when only one kind of species exists. In our case, where it appears that two complexes are formed, the fraction of intensity contributed by the 2 : 1 complex, $[B_3(I_0 - I_2)]$, must be subtracted from the total intensity to obtain the change in intensity due to the formation of the 1 : 1 complex, where B_3 is the normalized pre-exponential factor for the 2 : 1 complex in the fluorescence decay. Therefore the corrected expression for the evaluation of the overall association constant K_1 becomes [34]

$$\frac{1}{[(I_0 - I) - B_3(I_0 - I_2)]} = \frac{1}{(I_0 - I_1)} + \frac{1}{K_1(I_0 - I_1)[CD]} \quad (13)$$

where $(I_0 - I_2)$ can be obtained by extrapolating, to the y axis, plots of $1/(I_0 - I)$ vs. $1/[CD]$ (see Fig. 4). Fig. 6

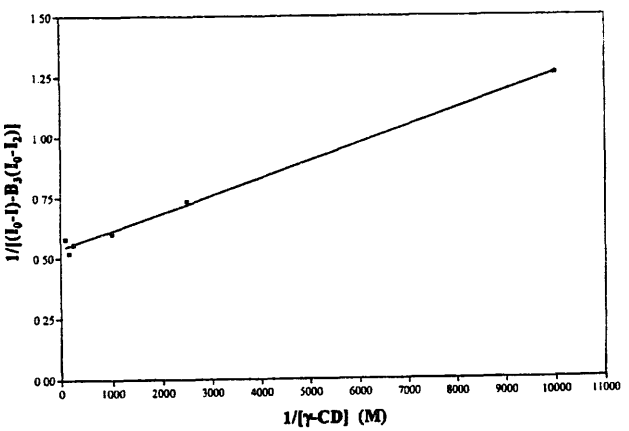

Fig. 6. Plot for molecule **2** complexed to γ-CD following the corrected Eq. (13).

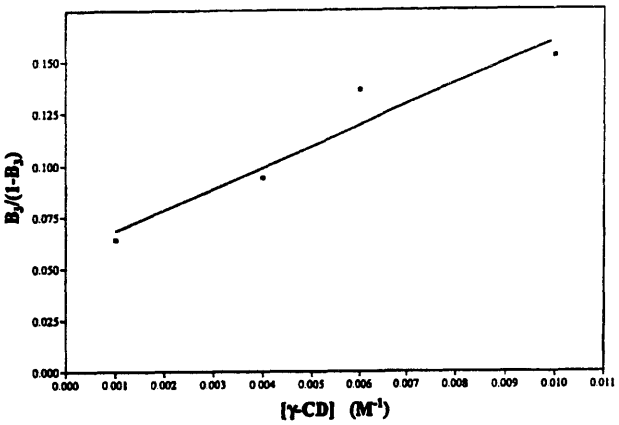

Fig. 7. Plot for molecule **2** complexed to γ-CD following Eq. (14).

depicts the linear plot described by Eq. (13) for molecule **2** in γ-CD from which the K_1 values are obtained. The overall formation constant for the 2 : 1 complex, as given in the equilibrium shown in Eq. (12), can be written as [34]

$$K_2 = \frac{S[CD]_2}{[SCD][CD]} = \frac{B_3}{(B_1+B_2)[CD]} = \frac{B_3}{(1-B_3)[CD]} \quad (14)$$

and can be obtained from the slope of a plot of $B_3/(1-B_3)$ vs. [CD] as in the above equation. Fig. 7 shows such a plot for molecule **2** in γ-CD.

Using the method described above, we have determined the association constants for molecules **1** and **2** in α- and γ-CDs, which are given in Table 3 together with the association constants determined by the steady state methods. As can be seen, there is excellent agreement between the values of K_1 determined by the two methods for both CD systems. In addition, we have determined the second association constants for α- and γ-CDs which could not be detected earlier by the steady state methods. The magnitude of the second association constant (K_2) is very small in γ-CD compared with K_1. This may be the reason why we were unable to detect the presence of the second complexed species in the steady state experiments. This result shows that the molecules associate with γ-CD in two different ways. The first complex is strong on the basis of the magnitude of the association constant and the second complex is very weak. This behaviour is very different from that in β-CD, where the second complex is the stronger of the two [46].

To obtain the decay associated spectra (DAS) of each of the species formed, we also studied the dependence of the fluorescence lifetime on the emission wavelength at a particular concentration of γ-CD (0.004 M in this case). We analysed the decay profiles at different wavelengths globally using the same procedure as for the concentration dependence. From the normalized pre-exponential factors, we calculated the fractional contribution to the fluorescence intensity of each species and, subsequently, using the steady state emission spectra, we recovered the DAS of the individual species. It should be noted that, for ground state equilibrium only, DAS and SAS (species associated spectra) have the same meaning [49]. Fig. 8 shows the DAS for molecule **1** in γ-CD. Thus it can be seen that the first complex formed (approximately 1.4 ns) is the main contributor to the total fluorescence intensity, whereas the second complex formed is the smallest contributor. This second complex is also largely red shifted relative to the fluorescence in water. This explains quite well the increase in bandwidth observed in the steady state fluorescence spectra when γ-CD is added to solutions of **1** and **2** (see Table 1). Such time-resolved spectra and global analysis have also recently been used to assess the existence of different emissive species in the observed fluorescence spectrum [56,57].

If we plot the fraction of molecules in water for **1** and **2** in α-CD (Table 4), an exponential form is obtained and the fraction reaches zero at approximately 0.1 M of α-CD. This result correlates well with the small equilibrium constants of the two complexes in α-CD. However, if we do the same for **1** and **2** in γ-CD, it becomes impossible to predict the convergence of the plots, since the maximum concentration of γ-CD that can be safely used is 0.01 M. Nevertheless, we can see from Table 4 that saturation is nearly attained at 0.01 M. This is not normal behaviour in view of the large equilibrium constants calculated with both steady state and time-resolved methods.

Since γ-CD is much less soluble than α-CD, an obvious artefact would be a contribution from light scattering to the close-to-resolution short lifetime component. Firstly, we checked that, at 0.01 M of γ-CD, all compounds are dissolved. Secondly, molecule **2**, which produces stronger complexes than molecule **1** in both CD systems, shows a lower contribution of the short lifetime component in both CDs. Thirdly, equilibrium constants were calculated by both steady state and time-resolved methods, and are approximately the same within experimental error limits. We thus believe that this possible artefact can be safely eliminated.

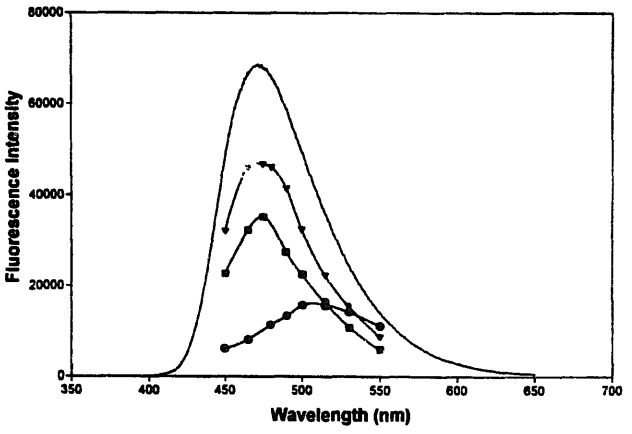

Fig. 8. Steady state fluorescence spectrum (λ_{exc} = 375 nm) and decay associated spectra (DAS) of molecule **1** in γ-CD (0.004 M): ■, 0.22 ns decay associated spectrum; ▼, 1.4 ns decay associated spectrum; ●, 5.0 ns decay associated spectrum. All points in the DAS were obtained by global analysis (global χ^2 = 1.11) and the lines are the cubic spline fitting of these data points.

It may be possible that, although Eqs. (6), (7), (13) and (14) seem to apply to Figs. 4–7, stoichiometric complexes may not be formed. We emphasized this possibility in Section 3.1, where a red edge effect was clearly shown, at least for molecule **1** in γ-CD (see Table 2), indicating that **1** forms complexes which may exist in many different conformations. We are currently working on this point.

4. Conclusions

The absorption and fluorescence studies of molecules **1** and **2**, together with lifetime measurements, show that they form complexes with α- and γ-CDs. Steady state experiments detect only one kind of complex, whereas time-resolved measurements reveal the presence of two kinds of complex. The results in α-CD are very similar to those in β-CD, but the interactions are much weaker. The two association constants have the same magnitude.

The results in γ-CD are different from those in α- and β-CDs. Unlike the fluorescence enhancement experienced in the latter systems, fluorescence quenching is observed in γ-CD. This has been related to a possible decrease in the quantum yield of the complexes formed. The association constants for the molecules in γ-CD are very high, but a number of the molecules always remain in the bulk water phase. This again is contrary to that observed in β-CD. The association constants for the second complex have been determined by time-resolved measurements; the values are always higher for molecule **2**, which has been correlated with the stronger hydrophobic nature of this molecule. The global analysis carried out in γ-CD at different wavelengths has enabled the DAS of the different species formed to be determined. This study shows that the size of the guest molecule and the restrictive environment of the host CD are the main driving forces behind complexation.

Acknowledgements

We gratefully acknowledge the financial assistance of the Natural Sciences and Engineering Research Council of Canada and the Fonds FCAR (Québec) in the form of grants. We thank Mr. Adrian Popowycz for the synthesis and purification of the substituted 3H-indoles studied here. We also wish to thank Dr. Michel Belletête and Dr. Prabir Kumar Pal for fruitful discussions.

References

[1] M.L. Bender and M. Komiyama, *Cyclodextrin Chemistry*, Springer-Verlag, New York, 1978.
[2] J. Szejtli, *Cyclodextrin Technology*, Kluwer Academic, Dordrecht, 1988.
[3] W. Saenger, *Angew. Chem., Int. Ed. Engl., 19* (1980) 344.
[4] J. Szejtli, *Cyclodextrins and Their Inclusion Complexes*, Akademiai Kiado, Budapest, 1982.
[5] S. Li and W.C. Purdy, *Chem. Rev., 92* (1992) 1457.
[6] R. Breslow, *Science, 218* (1982) 523.
[7] G. Marconi, S. Monti, B. Mayer and G. Köhler, *J. Phys. Chem., 99* (1995) 3943.
[8] M. Hoshino, M. Imamura, K. Ikehara and Y. Hama, *J. Phys. Chem., 85* (1981) 1820.
[9] T. Horozu, M. Hoshino and M. Imamura, *J. Phys. Chem., 86* (1982) 4426.
[10] S. Scypinsky and J.M. Drake, *J. Phys. Chem., 89* (1985) 2432.
[11] A. Örstan and J.B.A. Ross, *J. Phys. Chem., 91* (1987) 2739.
[12] G.C. Catena and F.V. Bright, *Anal. Chem., 61* (1989) 905.
[13] L. Flamigni, *J. Phys. Chem., 97* (1993) 9566.
[14] R.A. Dunbar and F.V. Bright, *Supramol. Chem., 3* (1994) 93.
[15] S. Hamai, *Bull. Chem. Soc. Jpn., 55* (1982) 2721.
[16] G.S. Cox, N.J. Turro, N.C. Yang and M.J. Chen, *J. Am. Chem. Soc., 106* (1984) 422.
[17] S. Hamai, *Bull. Chem. Soc. Jpn., 64* (1991) 431.
[18] S. Hamai and N. Mononobe, *J. Photochem. Photobiol. A: Chem., 91* (1995) 217.
[19] G.S. Cox, P.J. Hauptman and N. Turro, *J. Photochem. Photobiol. A: Chem., 39* (1984) 597.
[20] A. Nag, R. Dutta, N. Chattopadhyay and K. Bhattacharya, *Chem. Phys. Lett., 157* (1989) 83.
[21] K.A. Al-Hassan, *Chem. Phys. Lett., 227* (1994) 527.
[22] D.W. Cho, Y.H. Kim, S.G. Kang, M. Yoon and D. Kim, *J. Phys. Chem., 98* (1994) 558.
[23] G. Patonay, A. Shapira, P. Diamond and I.M. Warner, *J. Phys. Chem., 90* (1986) 1963.
[24] S. Hamai, *J. Phys. Chem., 94* (1990) 2595.
[25] T.C. Werner and I.M. Warner, *J. Incl. Phenom. Mol. Recog. Chem., 18* (1994) 385.
[26] B. Sarkar, U. Das, S. Bhattacharyya and S.K. Bose, *Bull. Chem. Soc. Jpn., 68* (1995) 1807.
[27] N. Chattoadhyay, T. Chakrabarty, A. Nag and M. Chowdhury, *J. Photochem. Photobiol. A: Chem., 52* (1990) 199.
[28] E.L. Roberts, P.T. Chou, T.A. Alexander, R.A. Agbaria and I.M. Warner, *J. Phys. Chem., 99* (1995) 5431.
[29] V. Ramamurthy and D.F. Eaton, *Acc. Chem. Res., 21* (1988) 300.
[30] S. Monti, L. Flamigni, A. Martelli and P. Bortolus, *J. Phys. Chem., 92* (1988) 4447.
[31] R.A. Agabaria, R. Uzan and D. Gill, *J. Phys. Chem., 93* (1989) 3855.
[32] Y. Kusumoto, *Chem. Phys. Lett., 136* (1987) 535.
[33] A. Muñoz de la Peña, T. Ndou, J.B. Zung and I.M. Warner, *J. Phys. Chem., 95* (1991) 3330.
[34] D.J. Jobe, R.E. Verrall, R. Palepu and V.C. Reinsborough, *J. Phys. Chem., 92* (1988) 3582.
[35] I.M. Warner, G. Patonay and G. Nelson, *Anal. Chem., 60* (1988) 274.
[36] V.K. Smith, T. Ndou and I.M. Warner, *J. Phys. Chem., 98* (1994) 8627.
[37] M. Belletête and G. Durocher, *J. Phys. Chem., 93* (1989) 1793.
[38] M. Belletête and G. Durocher, *J. Phys. Chem., 96* (1992) 9183.
[39] M. Belletête, R.S. Sarpal and G. Durocher, *Chem. Phys. Lett., 201* (1993) 145.
[40] R.S. Sarpal, M. Belletête and G. Durocher, *Can. J. Chem., 71* (1993) 1570.
[41] M. Belletête, R.S. Sarpal and G. Durocher, *Can. J. Chem., 72* (1994) 2239.
[42] M. Belletête, S. Nigam and G. Durocher, *J. Phys. Chem., 99* (1995) 4015.
[43] S. Nigam, M. Belletête, R.S. Sarpal and G. Durocher, *J. Lumin., 65* (1995) 65.
[44] S. Nigam, M. Belletête, R.S. Sarpal and G. Durocher, *J Chem. Soc., Faraday Trans., 91* (1995) 2133.
[45] S. Nigam, R.S. Sarpal, M. Belletête and G. Durocher, *J. Colloid Interface Sci., 177* (1996) 143.

[46] S. Nigam and G. Durocher, *J. Phys. Chem., 100* (1996) 7135.
[47] P. Skrabal, J. Steiger and H. Zellinger, *Helv. Chim. Acta, 58* (1975) 800.
[48] A. Popowycz, *M.Sc. Thesis*, Université de Montréal, 1992.
[49] Globals Unlimited, Version 1.02-2 (1990), updated in 1993, Laboratory for Fluorescence Dynamics, University of Illinois at Urbana-Champaign, 1993.
[50] D.W. Marquardt, *J. Soc. Ind. Appl. Math., 2* (1963) 431.
[51] K.A. Al-Hassan, U.K.A. Klein and A. Suwaiyan, *Chem. Phys. Lett., 212* (1993) 581.
[52] S. de Feyter, J. van Stam, N. Boens and F.C. de Schryver, *Chem. Phys. Lett., 249* (1996) 46.
[53] H.A. Benesi and J.H. Hildebrand, *J. Am. Chem. Soc., 71* (1949) 2703.
[54] Graph Pad Prism, Version 2.0 (1995), Graph Pad Software Inc., San Diego, CA, 1995.
[55] L.D. Janssens, N. Boens, M. Ameloot and F.C. de Schryver, *J. Phys. Chem., 94* (1990) 3564.
[56] P. Pal, H. Zeng, G. Durocher, D. Girard, R. Giasson, L. Blanchard, L. Gaboury and L. Villeneuve, *J. Photochem. Photobiol. A: Chem, 98* (1996) 65.
[57] A.M. Klock, W. Rettig, J. Hofkens, M. Van Damme and F.C. de Schryver, *J. Photochem. Photobiol. A: Chem., 85* (1995) 11.